Biosensors and Bioelectronics 34 (2012) 202–207

Contents lists available at SciVerse ScienceDirect

Biosensors and Bioelectronics

journal homepage: www.elsevier.com/locate/bios

Multi-wall carbon nanotube-polyaniline biosensor based on lectin–carbohydrate affinity for ultrasensitive detection of Con A

Fangxin Hu, Shihong Chen*, Chengyan Wang, Ruo Yuan*, Yun Xiang, Cun Wang

Education Ministry Key Laboratory on Luminescence and Real-Time Analysis, Key Laboratory of Chongqing Modern Analytical Chemistry, School of Chemistry and Chemical Engineering, Southwest University, Chongqing 400715, China

ARTICLE INFO

Article history:
Received 4 November 2011
Received in revised form 27 January 2012
Accepted 6 February 2012
Available online 14 February 2012

Keywords:
Concanavalin A
Multi-wall carbon nanotube
Polyaniline
D-Glucose
Lectin–carbohydrate affinity
Biosensor

ABSTRACT

In this paper, a novel method for detecting concanavalin A (Con A) was developed based on lectin–carbohydrate biospecific interactions. Multi-wall carbon nanotube-polyaniline (MWNT–PANI) nanocomposites, synthesized by in situ polymerization, were chosen to immobilize D-glucose through the Schiff-base reaction. The immobilized D-glucose showed high binding sensitivity and excellent selectivity to its target lectin, Con A. Cyclic voltammetry (CV), electrochemical impedance spectroscopy (EIS), transmission electron microscopy (TEM) and atomic force microscopy (AFM) were applied to characterize the assembly process of the modified electrode. Due to the high affinity of Con A for D-glucose and high stability of the propounded sensing platform, the fabricated biosensor achieved ultrasensitive detection of Con A with good sensitivity, acceptable reproducibility and stability. The changes of response current were proportional to the Con A concentrations from 3.3 pM to 9.3 nM, with a detection limit of 1.0 pM. Therefore, the combination of MWNT–PANI nanocomposites and the special binding force between lectin and carbohydrate provides an efficient and promising platform for the fabrication of bioelectrochemical devices.

1. Introduction

Concanavalin A (Con A), a member of the lectins family, has great effects on activation and proliferation of mature T cells (Pongracz et al., 2003). Meanwhile, it reveals several new insights into its regulatory function of the store-operated calcium cation entry on mouse immune cells in vitro (Ye et al., 2011). Con A is one of the most often studied lectins that exists as a dimer below pH 5.5, and a tetramer between pH 5.8 and 7.0 (molecular mass, 104,000 for tetramer) (Cella et al., 2010). Under neutral conditions, each subunit of Con A contains four binding sites (Yonzon et al., 2004). One is for calcium cation and manganese cation to activate the binding site of protein for carbohydrates, one is for hydrophobic recognition, the third one is specific for R-mannose or D-glucose residues, which belongs to the affinity between lectin and carbohydrate ligand.

Lectin binding of carbohydrate ligands, which has a high affinity comparable to that observed for antigen–antibody interactions, is special because the attractive forces at work are noncovalent, and the strength as well as specificity required for proper cellular targeting is great (Mann et al., 1998). Furthermore, this biospecific interaction can avoid the chemical denaturation of the biomolecular without any chemical modification during the binding of lectin and carbohydrate ligands (Li et al., 2011a,b). A lot researches concerning the lectin–carbohydrate affinity have been reported (Lebed et al., 2006; Bandaru et al., 2005; Geng et al., 2011). Besides, based on this well known fantastic force, a wide range of studies and applications in different types of biological assays have been done, such as, investigation of the carbohydrate and glycoprotein recognition processes (Boer et al., 2007; Nelson et al., 2004; Jiang et al., 2010), interpretation properties of malignant cells (Stoyloff and Ivanov, 2010), lectin structure elucidation (Pratap et al., 2002). Additionally, owing to the lectin–carbohydrate biospecific interactions between Con A and carbohydrates, the detection of carbohydrates have been reported (Cella et al., 2010; Li et al., 2011a,b). Similarly, Con A also can be detected with carbohydrates as recognition elements. Morokoshi and partners assembled glucose-carrying polymer chain on a colloidal Au-immobilized glass substrate as a sensing element to detect Con A by using a UV–vis spectrophotometer and its detection limit was 1.9 nM (Morokoshi et al., 2004). At present, many methods have been reported to detect Con A, such as UV–vis spectrophotometry (Guo et al., 2007), fluorescence technique (Huang et al., 2009), microarray imaging technique (Zhou and Zhou, 2006), and electrochemical method (Guo et al., 2008). Among various methods, the electrochemical method especially the electrochemical biosensor is promising for investigating biological binding assay because of its inherently rapid, simple, low-cost and miniaturized properties (Guo et al., 2008). However, detection

* Corresponding author. Tel.: +86 23 68253172; fax: +86 23 68253172.
E-mail addresses: cshong@swu.edu.cn (S. Chen), yuanruo@swu.edu.cn (R. Yuan).

0956-5663/$ – see front matter © 2012 Elsevier B.V. All rights reserved.
doi:10.1016/j.bios.2012.02.003

of Con A by electrochemical biosensor was still at a very early stage. Guo et al. (2008) immobilized functionalized vesicles composed of glycolipid and alkanethiol lipids onto gold surface to construct an electrochemical biosensor for Con A detection, with $K_3Fe(CN)_6$ as electron-shuttling mediators. Bai et al. (2009) constructed an electrochemical impedance spectroscopy biosensor to detect Con A with D-mannose as the recognition element, and a detection limit of 0.67 nM was obtained. Hence, it is very attractive to develop a simple and effective strategy for fabricating a mediated-free electrochemical biosensor to achieve the ultrasensitive detection of Con A.

In order to construct an amperometric transducer biosensor, it is quite important to immobilize the recognition elements onto the electrode to provide the sites of molecular recognition. But the efficient immobilization of D-glucose on electrode surface is always a challenge, so a prominent underlying substrate is needed. Since their discovery in 1960, conducting polymers (CP) have been an attractive research subject because of their interesting properties and numerous application possibilities (Bhadra et al., 2009). Polyaniline (PANI) is a typical CP due to its high conductivity, unique redox properties, good environmental stability, ease of synthesis, and unusual doping/dedoping chemistry (Wu et al., 2010, Garai and Nandi, 2009). Additionally, PANI provides a suitable matrix for the immobilization of biomolecules (Wan et al., 2010), and nanostructured PANI offers higher effective surface area and shorter penetration depth for target molecules in biosensor applications (Huang and Kaner, 2004). However, the mechanical weakness and poor solubility of PANI might be a great obstacle for its experimental investigations and commercial exploitation (Shao et al., 2010). Thus, the introduction of multi-wall carbon nanotube (MWNT) with excellent mechanical and electronic properties (Bhandari et al., 2009) may provide an effective means to improve the mechanical weakness of PANI. Moreover, as hybrid nanomaterials, the MWNT–PANI nanocomposites exhibited unique optical, electrical, magnetic, and chemical properties, with better catalytic activity and enhanced electrical conductivity (Cao et al., 2010; Tang et al., 2011). Actually, MWNT–PANI nanocomposites have already been used in many biosensors, for example, Srivastava et al. (2009) reported MWNT–PANI composites thin films for hydrogen gas sensing applications. Huan et al. (2011) carried out the sensitive detection of an Anthrax biomarker using a glassy carbon electrode with MWNT–PANI–peptide composites. Thus, MWNT–PANI nanocomposites were chosen as the immobilization material for its possibility to modify D-glucose on the electrode through Schiff-base reaction.

In this paper, a novel biosensor was constructed for ultrasensitive detection of Con A which depended on the specific affinity of Con A to D-glucose. MWNT–PANI nanocomposites acted as the electron transfer mediator as well as immobilization material for D-glucose. They were synthesized by in situ polymerization with potassium persulfate (KPS) as oxidant in the presence of MWNT under the acidic environment and were characterized through transmission electron microscopy (TEM). After D-glucose was covalently immobilized on the electrode, bovine serum albumin (BSA) was chosen to eliminate non-specific binding effect. The assembly processes were investigated by cyclic voltammetry (CV), electrochemical impedance spectroscopy (EIS) and atomic force microscopy (AFM). Due to the excellent electrical conductivity of MWNT–PANI nanocomposites and the lectin–carbohydrate biospecific interaction, the as-prepared Con A biosensor endowed low detection limit and relatively wider linear range through a sensitive differential pulse voltammetry (DPV) detection method. Meanwhile, the stability and sensitivity of the biosensor are greatly improved because Con A contains multiple sites with high affinity for the attachment of the D-glucose.

2. Experimental

2.1. Reagents and chemicals

Concanavalin A (Con A) from *Canavalia ensiformis* (jack bean), aniline and bovine serum albumin (BSA, 96–99%) were all purchased from Sigma. Multi-wall carbon nanotube (MWNT > 95% purity) were purchased from Chengdu Organic Chemicals Co. Ltd. and purified by refluxing in concentrated nitric acid for 7 h prior to use. D-Glucose, potassium persulfate (KPS, $K_2S_2O_8$) were obtained from Shanghai Chemical Reagent Co. All the other chemicals employed were analytical grade and were used as received. 0.1 M phosphate buffer solutions (PBS) with various pH were prepared by using the stock solutions of 0.1 M Na_2HPO_4 and 0.1 M KH_2PO_4. The supporting electrolyte was 0.1 M KCl. Double-distilled water was used throughout the experiments. The different concentrations of Con A solution were prepared with 0.1 M pH 7.0 PBS containing 1 mM $CaCl_2$ and 1 mM $MnCl_2$.

2.2. Apparatus

CV, EIS and DPV were carried out on CHI 660D electrochemical workstation (CH Instruments, Chenhua Corp., China). The conventional three-electrode system involved modified electrodes as working electrode, a platinum wire as auxiliary electrode and a saturated calomel as reference electrode (SCE). AFM images were taken using scanning probe microscope (Vecco, USA). TEM was obtained by using a H600 TEM (Hitachi, Japan).

2.3. Synthesis of MWNT–PANI nanocomposites

In this strategy, MWNT–PANI nanocomposites were synthesized according to the literature (Srivastava et al., 2009, Zhang et al., 2011) with some modification. Briefly, under constant stirring, 0.3 mM freshly distilled aniline was dissolved in 10 mL of 0.5 M H_2SO_4 solution portion by portion. Subsequently, 3.0 mg MWNT were dispersed into the above aniline/H_2SO_4 solution for 20 h to adsorb aniline monomer on the nanotubes. Later, the polymerization reaction was carried out at 0 °C for 8 h with the help of KPS (0.15 M) solution. At last, the MWNT–PANI nanocomposites were centrifuged, washed in double-distilled water and ethanol, respectively.

2.4. Preparation of the Con A biosensors

The glassy carbon electrode (GCE) was carefully polished by 0.3 and 0.05 μm alumina. Then, it was sonicated successively with distilled water and ethanol for 5 min until a mirror like surface was obtained.

Firstly, 8 μL MWNT–PANI suspension (2.0 mg mL^{-1}), dispersed in double-distilled water with the aid of ultrasonic, was dropped on the clean GCE surface to obtain the MWNT–PANI/GCE. Then D-glucose was modified on the electrode under 50 °C for 6 h through Schiff-base reaction. Finally, BSA (0.5%) was applied to block the remaining active sites and eliminate non-specific binding effect. The preparation process of the modified electrode is shown in Scheme 1. The modified electrode (BSA/D-glucose/MWNT–PANI/GCE) was stored at 4 °C when not in use.

2.5. Experimental measurements

The CV was carried out in 0.1 M PBS (pH 6.5). The EIS was carried out in the presence of a 5.0 mM $K_3[Fe(CN)_6]/K_4[Fe(CN)_6]$ (1:1) mixture as a redox probe at a bias potential of 0.17 V. The frequency range was 50 MHz to 10 kHz.

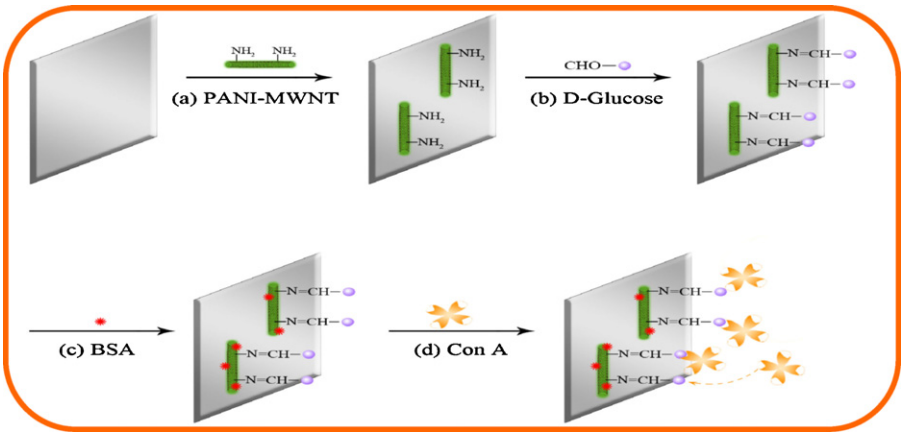

Scheme 1. Illustration of the preparation process of Con A biosensor.

After the biosensor (BSA/D-glucose/MWNT–PANI/GCE) was incubated in 50 μL incubation solution containing different concentrations of Con A at 4 °C for 40 min and then washed carefully with doubly distilled water, the DPV measurements were carried out in unstirred 3 mL 0.1 M PBS (pH 6.5) with the potential range from −0.5 to +0.5 V, pulse amplitude of 50 mV and width of 50 ms. The detection is based on the change of DPV peak currents before and after the Con A–D-glucose reaction. When the background signal was stabilized, the current response was recorded as I_0. After Con A was incubated onto the electrode, the Con A–D-glucose complex coating on the electrode surface inhibited the electron transfer and led to the decrease of the DPV peak current, which was recorded as I. The current change was calculated by Eq. (1):

$$\Delta I = I_0 - I$$

3. Results and discussion

3.1. The characterization of the modified electrode

3.1.1. TEM characterization of the MWNT and MWNT–PANI nanocomposites

Fig. 1 depicted the TEM micrographs of pure MWNT and the MWNT–PANI nanocomposites, respectively. Twisted and wrapped fibrillar network morphology belonging to MWNT could be distinctly observed in Fig. 1a. It can be found in Fig. 1b that many new branches are attached on MWNT surfaces, which is attributed to the coating of PANI onto MWNT surfaces. For a comparison between pure MWNT and MWNT–PANI nanocomposites morphology, the latter one was obviously thicker than the former one. The average diameter of nanotubes increased from 15 ± 3 nm (Fig. 1a) to 25 ± 3 nm (Fig. 1b), indicating that the inorganic–organic nanocomposites were formed.

3.1.2. AFM characterization of the modified electrode

The surface topographies of MWNT–PANI and Con A/BSA/D-glucose/MWNT–PANI films were analyzed by AFM and the images were shown in Fig. 2a and b, respectively. Tubular structures can be found in Fig. 2a, which indicates the existence of MWNT–PANI. After D-glucose, BSA and Con A were assembled onto the MWNT–PANI film as shown in Fig. 2b, the tubular morphology of MWNT–PANI turned blurry and the whole scene became smooth, dense and compact.

3.1.3. Electrochemical characterization of the modified electrode

The CV was applied to characterize different electrodes. Fig. 3A presents the cyclic voltammograms (CVs) of the electrode at every stage. As shown in Fig. 3A, no redox peaks appeared on the bare electrode (curve a). However, after the GCE was modified with MWNT–PANI nanocomposites, a pair of stable and well-defined redox peaks at 0.04 V and −0.17 V vs. SCE was observed (curve b). This might be due to the excellent redox-activity of MWNT–PANI nanocomposites materials. Generally, there are three redox forms of PANI: fully oxidized state pernigraniline (PG), fully reduced state leucoemeraldine (LE) and half oxidized/half reduced state emeraldine (EB) (Premamoy et al., 1999; Dhand et al., 2010a,b). Redox

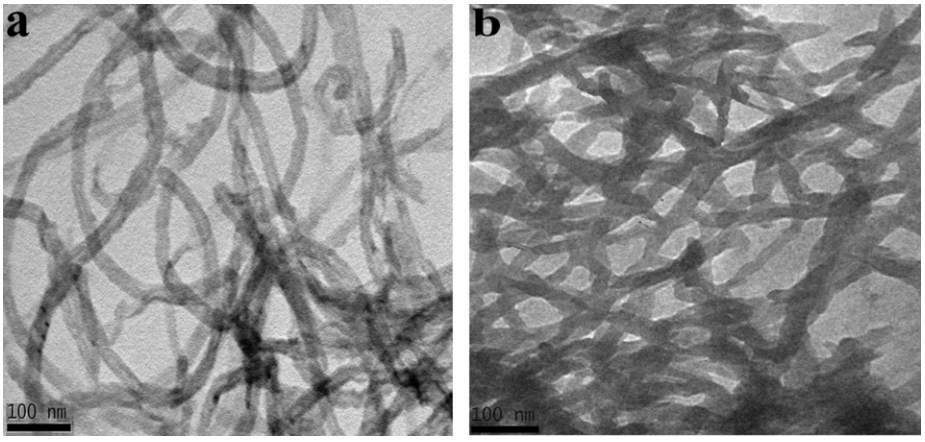

Fig. 1. TEM images of MWNT (a) and MWNT–PANI (b) modified films.

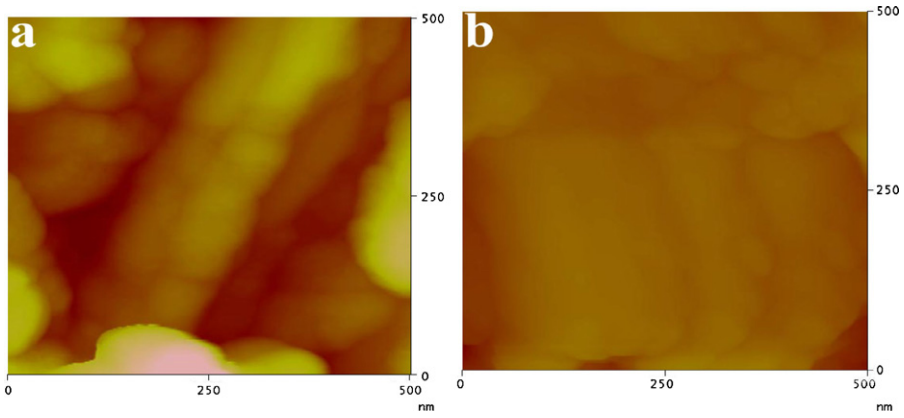

Fig. 2. AFM images of MWNT–PANI (a) and Con A/BSA/D-glucose/MWNT–PANI (b) modified films.

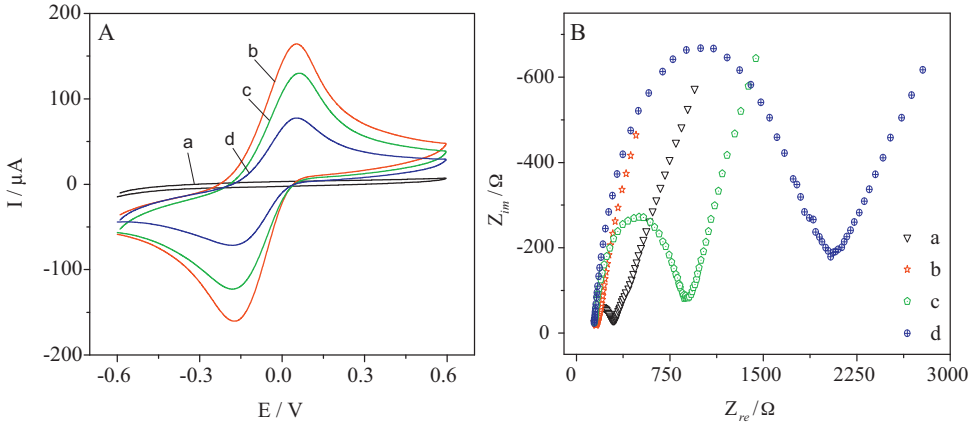

Fig. 3. CVs in 0.1 M PBS (pH 6.5) at a scan rate of 50 mV s^{-1} (A) and EIS in 5 mM $K_3[Fe(CN)_6]/K_4[Fe(CN)_6]$ solution (B) at the bare electrode (a), MWNT–PANI/GCE (b), D-glucose/MWNT–PANI/GCE (c) and BSA/D-glucose/MWNT–PANI/GCE (d), respectively.

reaction take place along with the transform of PANI from EB state to LE state (Dhand et al., 2010a,b). The peak potential of 0.04 V and −0.17 V observed at MWNT–PANI/GCE in this project is lower than that of 0.2 V and 0 V for pure PANI observed by Trung et al. (2005). This might due to the addition of MWNT in the MWNT–PANI nanomaterials and the influence of pH value of the test solution. On one hand, dopants in the PANI composites may induce the shift of the peak potentials. As reported by Trung et al. (2005), the addition of Ni to PANI induced its redox peak potentials shift from 0.2 V and 0 V to about 0.05 V and −0.1 V. On the other hand, pH value of the test solution would also influence the peak potentials of the PANI composites. Dhawan et al. investigated the influence of pH on the CV behaviors of polyaniline film on ITO electrode. The result showed that the redox peaks of PANI shifted to the negative value gradually with the increase of pH value of test solution (Dhawan et al., 1997). Compared to curve b, the peak current of curve c was obviously decreased, indicating that D-glucose has been modified on the biosensor through Schiff-base reaction. The decrease of peak current was due to the insulation of D-glucose. After adsorbing BSA, the peak current decreased further because BSA was nonconducting, as can be observed in curve d.

EIS measurements were also applied to characterize the interface properties of surface-modified biosensors. Generally, the high frequency region of the impedance plot presents a semicircle, which corresponds to the electron-transfer-limited process and the semicircle diameter equals the electron-transfer resistance (R_{et}) of the redox probe $[Fe(CN)_6]^{3-/4-}$. The Warburg line in the low frequency region corresponds to the diffusion step of the overall process (Zhuo et al., 2009). As shown in Fig. 3B, an obvious semicircular domain with the diameter of 153 Ω can be found in curve a, indicating the resistance of bare electrode. There is a sharp decrease of the resistance after modification of the MWNT–PANI nanocomposites, shown in curve b. An interesting phenomenon can be observed in curve c that the diameter of semicircular domain has an obvious increase to 736 Ω when D-glucose was decorated onto the MWNT–PANI film. This can be attributed to the non-conductive properties of D-glucose. Similarly, the inhibition effect of the BSA for electron transfer made the resistance of the modified electrode increase to 1906 Ω (curve d).

3.2. Optimization of experimental parameters

In order to obtain an optimal condition for the biosensor (BSA/D-glucose/MWNT–PANI/GCE) to detect Con A, selections were carried out involving pH of the detection solution and incubation time of the biosensor in Con A solutions.

As is known to all, the pH value of the electrolyte is important for the performance of the biosensor. Hence, we studied the influence of pH on the behavior of the working electrode. After the biosensor was incubated in 0.3 nM Con A solution for 40 min, DPV response was measured at a series of pH values of the detection solution. From 4.5 to 6.5, DPV response current of the biosensor decreased with the increase of pH value. However, from 6.5 to 9.0, DPV response current began to increase as shown in Fig. 4A. Taking account of the peak current response as well as the condition of specific binding affinity of D-glucose and Con A, pH 6.5 was selected for further experiments.

The effect of incubation time was investigated by detecting DPV response of the BSA/D-glucose/MWNT–PANI/GCE in 0.1 M PBS (pH 6.5) after immersion in 0.3 nM Con A solution for 10, 20, 40 and

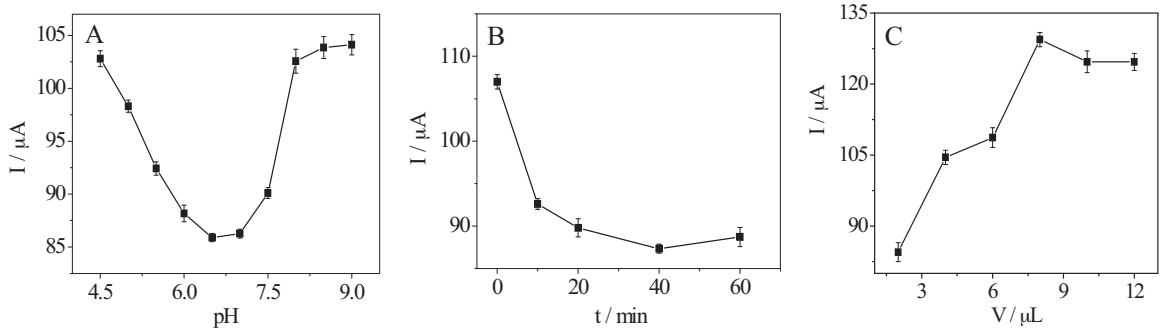

Fig. 4. Dependence of the DPV response of BSA/D-glucose/MWNT–PANI/GCE to 0.3 nM Con A on the pH of PBS at an incubation time of 40 min (A) and on the incubation time in 0.1 M PBS (pH 6.5) (B). Dependence of the DPV response of MWNT–PANI/GCE on the amount of MWNT–PANI composites (C).

60 min, respectively. The relationship between incubation time and the DPV peak current was shown in Fig. 4B. Apparently, the DPV peak current showed a rapid decrease with the increase of incubation time before 40 min. With the time up to 40 min, there was no obvious decrease, which indicated an equilibration state was reached. Therefore, the incubation time of 40 min was adopted in subsequent work.

The dependence between the current response and the amount of redox marker was investigated in detail. As shown in Fig. 4C, The current response of the biosensor increased with the increase of the amount of MWNT–PANI suspension from 2 μL to 8 μL, and slightly decreased when the amount exceed 8 μL. Thus, 8 μL was selected for further modification of electrode.

3.3. Performance of the biosensor

The performance of the proposed biosensor was evaluated by using DPV technique to detect Con A under the optimization conditions. Curve a in Fig. 5A displayed the DPV response of the biosensor to zero Con A, which was obtained after several successive scan until the DPV signal of the biosensor was stable, and this current signal was defined as the baseline signal (I_0). The DPV peak currents (I) of the biosensor after the Con A–D-glucose reaction showed a decrease with increasing Con A concentrations in the incubation solution, as shown in Fig. 5A curve b to curve h. The reason for this might be that the incubation of the biosensor with Con A solution resulted in the formation of Con A–D-glucose complex, which hindered the electron transfer between the electrode and the MWNT–PANI nanocomposites since Con A–D-glucose complex was non-conductive. The calibration plots were obtained by recording the changes of the DPV peak current vs. the different concentrations of Con A solutions according to Eq. (1). When the Con A concentration varied from 3.3 pM to 9.3 nM, the ΔI was proportional to the Con A concentration (shown in the inset of Fig. 5A) and the regression equation was expressed as ΔI (μA) = 8.3147 + 0.0013 $C_{Con\,A}$ (pM) (n = 7), with a correlation coefficient of 0.998. The detection limit of the proposed biosensor was 1.0 pM, which was estimated from the expression of $3S/K$ (where S is the standard deviation for 10 determinations of blank solution and K is the slope of the calibration plot) (Shi et al., 2005). The obtained detection limit for Con A was obviously lower than some reported values, such as 75.00 pM (Huang et al., 2009), 0.10 nM (Guo et al., 2007) or 0.13 nM (Lyu et al., 2008).

3.4. Reproducibility, stability and selectivity of the Con A biosensor

The baseline is the key factor in this work since the reduction current ($\Delta I = I_0 - I$) is treated based on the baseline current (I_0). In this project, the concentration and volume of MWNT–PANI suspension modified on the electrode was constant to ensure the consistency of the redox marker quantity modified on the electrode.

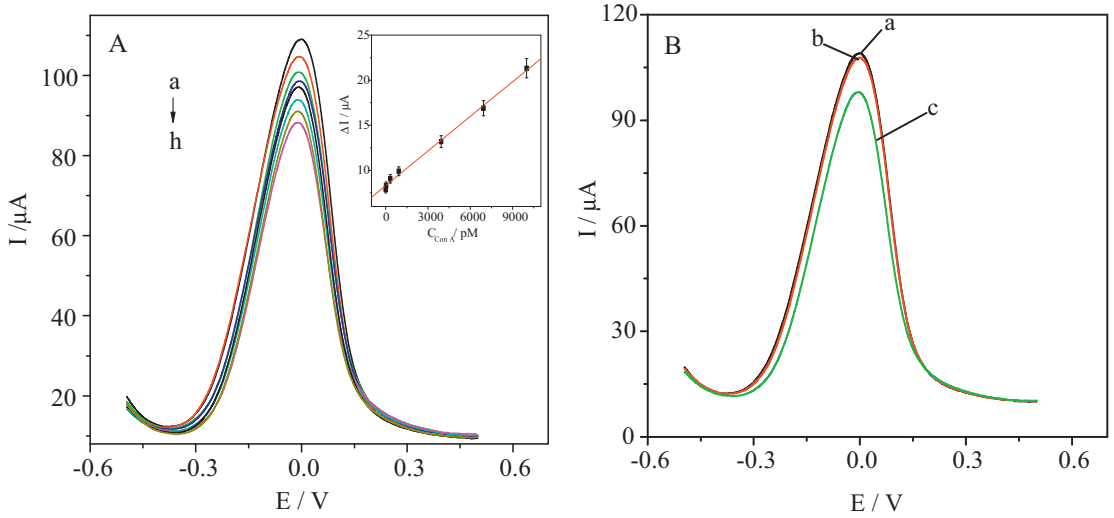

Fig. 5. (A) DPV response of BSA/D-glucose/MWNT–PANI/GCE to various concentrations of Con A in 0.1 M PBS (pH 6.5) after 40 min incubation, from a to h: 0, 3.3 pM, 33.3 pM, 0.3 nM, 0.9 nM, 3.3 nM, 6.9 nM and 9.3 nM. Inset: linear calibration curve. (B) DPV responses of BSA/D-glucose/MWNT–PANI/GCE before (curve a) and after incubation 1% BSA (curve b) and 0.3 nM Con A (curve c) in 0.1 M PBS (pH 6.5), respectively.

Thus, the baseline, namely, the DPV signal obtained at the electrodes which were fabricated with the same process was almost invariable. The reproducibility of the baseline was evaluated by assaying five biosensors prepared independently with the same fabrication procedure. The reproducibility is acceptable with a relative standard deviation (R.S.D.) of 2.1%. The reproducibility of the biosensor for detecting Con A was also investigated. The R.S.D. for five biosensors prepared independently with the same fabrication procedure were 6.9% and 6.0% at the Con A concentrations of 33.3 pM and 0.3 nM, respectively. The results suggested that an acceptable reproducibility in its linear range was obtained at the biosensor.

The stability of the baseline was investigated through successive DPV measurements at the same biosensor in working buffer, a R.S.D. of 1.6% for six measurements was obtained. Furthermore, the storage stability of the proposed biosensor was also studied. The electrode was suspended above 0.1 M PBS at 4 °C in a refrigerator when not in use. DPV was applied to measure the response of the biosensor to 0.3 nM Con A intermittently. The biosensor lost about 6.0% and 10.0% of its original response after 10 days and 20 days, respectively, indicating an acceptable stability. This might be due to the fact that MWNT–PANI nanocomposites, possessing high effective surface area and strong electrical conductivity, offered a favorable immobilization platform for D-glucose.

In order to testify the special binding effect between Con A and D-glucose, specificity detection was performed by detecting DPV responses of BSA/D-glucose/MWNT–PANI/GCE to 1% BSA and 0.3 nM Con A, respectively. Fig. 5B showed that the BSA/D-glucose/MWNT–PANI/GCE did not exhibit obvious response to BSA (curve b) compared with the baseline (curve a) and the response current to BSA was almost negligible in consideration of such a high response to Con A (curve c), suggesting that the active sites on the electrode had been blocked out and the response of BSA/D-glucose/MWNT–PANI/GCE to Con A is based on the special binding effect between Con A and D-glucose.

4. Conclusion

A novel, convenient and versatile MWNT–PANI electrochemical biosensor grounded on lectin–carbohydrate biospecific interactions was fabricated to detect Con A. MWNT–PANI nanocomposites which possessed excellent electro-activity were selected as the electron transfer mediator and immobilization material for D-glucose. The combination of the virtues of MWNT–PANI nanocomposites and sensitive DPV measurement technique gained the ultrasensitive detection of Con A at proposed biosensor. Furthermore, the biosensor possessed low detection limit, acceptable reproducibility and stability. Thus, such a specific binding force between lectin and carbohydrate shows the prospect of the biosensor in lectin sensing or carbohydrate sensing and provides an efficient and promising platform for the fabrication of bioelectrochemical devices.

Acknowledgments

This work was supported by the National Natural Science Foundation of China (21075100), Key Lab of Chongqing Modern Analytical Chemistry, Chongqing Municipal Key Laboratory on Luminescence and Real-Time Analysis, Southwest University, the Doctor Foundation of Southwest University (SWUB2008048) and the Fundamental Research Funds for the Central Universities (XDJK2009C082 and XDJK2012A004).

References

Bai, X.F., Qi, H.L., Gao, Q., Zhang, C.X., 2009. Chin. J. Anal. Chem. 37, E120.
Bandaru, N.M., Sampath, S., Jayaraman, N., 2005. Langmuir 21, 9591–9596.
Bhadra, S., Khastgir, D., Singha, N.K., Lee, J.H., 2009. Prog. Polym. Sci. 34, 783–810.
Bhandari, S., Deepa, M., Srivastava, A.K., Joshi, A.G., Kant, R., 2009. J. Phys. Chem. B 113, 9416–9428.
Boer, A.R., Hokke, C.H., Deelder, A.M., Wuhrer, M., 2007. Anal. Chem. 79, 8107–8113.
Cao, L.Y., Liu, Y.L., Zhang, B.H., Lu, L.H., 2010. ACS Appl. Mater. Interfaces 2, 2339–2346.
Cella, L.N., Chen, W., Myung, N.V., Mulchandani, A., 2010. J. Am. Chem. Soc. 132, 5024–5026.
Dhand, C., Das, M., Datta, M., Malhotra, B.D., 2010a. Biosens. Bioelectron. 26, 2811–2821.
Dhand, C., Das, M., Sumana, G., Srivastava, A.K., Pandey, M.K., Kim, C.G., Datta, M., Malhotra, B.D., 2010b. Nanoscale 2, 747–754.
Dhawan, S.K., Kumar, D., Ram, M.K., Chandra, S., Trivedi, D.C., 1997. Sens. Actuators B 40, 99–103.
Garai, A., Nandi, A.K., 2009. Synth. Met. 159, 1710–1716.
Geng, J., Biedermann, F., Zayed, J.M., Tian, F., Scherman, O.A., 2011. Macromolecules 44, 4276–4281.
Guo, C.X., Boullanger, P., Jiang, L., Liu, T., 2007. Biosens. Bioelectron. 22, 1830–1834.
Guo, C.X., Boullanger, P., Jiang, L., Liu, T., 2008. Colloid Surf. B 62, 146–150.
Huang, C.C., Chen, C.T., Shiang, Y.C., Lin, Z.H., Chang, H.T., 2009. Anal. Chem. 81, 875–882.
Huang, J.X., Kaner, R.B., 2004. J. Am. Chem. Soc. 126, 851–855.
Huan, T.N., Ganesh, T., Han, S.H., Yoon, M.Y., Chung, H., 2011. Biosens. Bioelectron. 26, 4227–4230.
Jiang, X.Z., Housni, A., Gody, G., Boullanger, P., Charreyre, M.T., Delair, T., Narain, R., 2010. Bioconjug. Chem. 21, 521–530.
Lebed, K., Kulik, A.J., Forró, L., Lekka, M., 2006. J. Colloid Interfaces Sci. 299, 41–48.
Li, F., Feng, Y., Yang, L.M., Li, L., Tang, C.F., Tang, B., 2011a. Biosens. Bioelectron. 26, 2489–2494.
Li, W.J., Yuan, R., Chai, Y.Q., Zhong, H.A., Wang, Y., 2011b. Electrochim. Acta 56, 4203–4208.
Lyu, Y.K., Lim, K.R., Lee, B.Y., Kim, K.S., Lee, W.Y., 2008. Chem. Commun., 4771–4773.
Mann, D.A., Kanai, M., Maly, D.J., Kiessling, L.L., 1998. J. Am. Chem. Soc. 120, 10575–10582.
Morokoshi, S., Ohhori, K., Mizukami, K., Kitano, H., 2004. Langmuir 20, 8897–8902.
Nelson, A., Belitsky, J.M., Vidal, S., Joiner, C.S., Baum, L.G., Stoddart, J.F., 2004. J. Am. Chem. Soc. 126, 11914–11922.
Pongracz, J., Parnell, S., Anderson, G., Jaffrézou, J.P., Jenkinson, E., 2003. Mol. Immunol. 39, 1013–1023.
Pratap, J.V., Jeyaprakash, A.A., Rani, P.G., Sekar, K., Surolia1, A., Vijayan, M., 2002. J. Mol. Biol. 317, 237–247.
Premamoy, G., Samir, K.S., Amit, C., 1999. Eur. Polym. J. 35, 699–710.
Shao, D.D., Hu, J., Chen, C.L., Sheng, G.D., Ren, X.M., Wang, X.K., 2010. J. Phys. Chem. C 114, 21524–21530.
Shi, Q.C., Peng, T.Z., Zhu, Y.N., Yang, C.F., 2005. Electroanalysis 17, 857–861.
Srivastava, S., Sharma, S.S., Kumar, S., Agrawal, S., Singh, M., Vijay, Y.K., 2009. Int. J. Hydrogen Energy 34, 8444–8450.
Stoyloff, J., Ivanov, S., 2010. Brain Res. Bull. 83, 65–75.
Tang, J., Tang, D.P., Su, B.L., Huang, J.X., Qiu, B., Chen, G.N., 2011. Biosens. Bioelectron. 26, 3219–3226.
Trung, T., Trung, T.H., Chang, S.H., 2005. Electrochim. Acta 51, 984–990.
Wan, D., Yuan, S.J., Li, G.L., Neoh, K.G., Kang, E.T., 2010. ACS Appl. Mater. Interfaces 2, 3083–3091.
Wu, Q., Xu, Y.X., Yao, Z.Y., Liu, A.R., Shi, G.Q., 2010. ACS Nano 4, 1963–1970.
Ye, Y.X., Zhang, Y.X., Lu, X.Y., Huang, X.Y., Zeng, X.F., Lai, X.Q., Zeng, Y.Y., 2011. Immunobiology, doi:10.1016/j.imbio.2011.03.001.
Yonzon, C.R., Jeoung, E., Zou, S.L., Schatz, G.C., Mrksich, M., Duyne, R.P.V., 2004. J. Am. Chem. Soc. 126, 12669–12676.
Zhang, Y.J., Lin, Y.W., Chang, C.C., Wu, T.M., 2011. Synth. Met. 161, 937–942.
Zhou, X.C., Zhou, J.Z., 2006. Biosens. Bioelectron. 21, 1451–1458.
Zhuo, Y., Yuan, P.X., Yuan, R., Chai, Y.Q., Hong, C.L., 2009. Biomaterials 30, 2284–2290.